

A thermo-responsive and photo-polymerizable chondroitin sulfate-based hydrogel for 3D printing applications

A. Abbadessa^a, M.M. Blokzijl^{a,b}, V.H.M. Mouser^b, P. Marica^a, J. Malda^{b,c}, W.E. Hennink^a, T. Vermonden^{a,*}

^a Department of Pharmaceutics, Utrecht Institute for Pharmaceutical Sciences (UIPS), Faculty of Science, Utrecht University, P.O. Box 80082, 3508 TB Utrecht, The Netherlands

^b Department of Orthopedics, University Medical Center Utrecht, P.O. Box 85500, 3508 GA Utrecht, The Netherlands

^c Department of Equine Sciences, Faculty of Veterinary Medicine, Utrecht University, P.O. Box 80163, 3508 TD Utrecht, The Netherlands

ARTICLE INFO

Article history:

Received 24 December 2015

Received in revised form 12 April 2016

Accepted 18 April 2016

Available online 22 April 2016

Keywords:

Methacrylated chondroitin sulfate

Thermo-sensitive hydrogel

Photo-polymerization

Shear thinning

Cartilage 3D printing

ABSTRACT

The aim of this study was to design a hydrogel system based on methacrylated chondroitin sulfate (CSMA) and a thermo-sensitive poly(*N*-(2-hydroxypropyl) methacrylamide-mono/dilactate)-polyethylene glycol triblock copolymer (M₁₅P₁₀) as a suitable material for additive manufacturing of scaffolds. CSMA was synthesized by reaction of chondroitin sulfate with glycidyl methacrylate (GMA) in dimethylsulfoxide at 50 °C and its degree of methacrylation was tunable up to 48.5%, by changing reaction time and GMA feed. Unlike polymer solutions composed of CSMA alone (20% w/w), mixtures based on 2% w/w of CSMA and 18% of M₁₅P₁₀ showed strain-softening, thermo-sensitive and shear-thinning properties more pronounced than those found for polymer solutions based on M₁₅P₁₀ alone. Additionally, they displayed a yield stress of 19.2 ± 7.0 Pa. The 3D printing of this hydrogel resulted in the generation of constructs with tailorable porosity and good handling properties. Finally, embedded chondrogenic cells remained viable and proliferating over a culture period of 6 days. The hydrogel described herein represents a promising biomaterial for cartilage 3D printing applications.

© 2016 Elsevier Ltd. All rights reserved.

1. Introduction

Tissue-engineered constructs are currently under investigation for the regeneration of several types of tissue, including bony, cartilaginous and vascular tissues. A tissue engineering (TE) approach is of particular relevance for damaged tissues that have a poor

capability to regenerate spontaneously, such as articular cartilage defects of critical sizes. Biomimetic hydrogels composed of naturally occurring polysaccharides, e.g. chondroitin sulfate (CS) and hyaluronic acid (HA) have already shown significant chondrogenic potential for encapsulated chondrocytes and mesenchymal stem cells (Chung, Beecham, Mauck, & Burdick, 2009; Erickson et al., 2009; Hu, Li, Zhou, & Gao, 2011; Ko, Huang, Huang, & Chu, 2009; Levett et al., 2014; Na et al., 2007; Toh, Lim, Kurisawa, & Spector, 2012; Yoo, Lee, Yoon, & Park, 2005). Hence, they are promising biopolymers for the development of implantable scaffolds in TE. In native tissue, CS is predominantly present as part of aggrecan and this natural polymer is involved in several biological mechanisms for the physiological maintenance of cartilage and its role in the resistance to compressive loading. More specifically, due to its hydrophilic nature and abundant negative charges, CS is responsible for retaining a large amount of water in the extracellular matrix (ECM), which is partially released upon compression and re-absorbed when the load is removed (Roughley & Mort, 2014). This mechanism not only provides mechanical resistance, but also contributes to the nutrients/waste products exchange, and thereby also to functioning/performance of the embedded chondrocytes.

Abbreviations: bFGF, recombinant human Fibroblast Growth Factor-basic; CS, chondroitin sulfate; CS-TBA, CS in form of TBA salt; CSMA, methacrylated CS; CP, Cloud Point; DAPI, 4',6-diamidino-2-phenylindole; DM, degree of methacrylation; DMAP, 4-(*N,N*-dimethylamino)pyridine; DMEM/F-12, Dulbecco's Modified Eagle Medium Nutrient Mixture F-12 supplemented with GlutaMax-1 31331; DMSO, dimethyl sulfoxide; EdU, 5-ethynyl-2'-deoxyuridine; GMA, glycidyl methacrylate; ¹H NMR, ¹H-Nuclear Magnetic Resonance; HA, hyaluronic acid; MA, methacrylic anhydride; M₁₅P₁₀, methacrylated poly(*N*-(2-hydroxypropyl) methacrylamide-mono/dilactate)-PEG triblock; Mn, number average molecular weight; Mp, peak molecular weight; PBS, Phosphate buffered saline; PDI, polydispersity index; PEG, polyethylene glycol; pen/strep, penicillin/streptomycin; pHPMALac, poly(*N*-(2-hydroxypropyl) methacrylamide-mono/dilactate); ratio TBA, CS molar ratio of TBA per disaccharide units of CS; TBA, tetrabutylammonium; T_{gel}, temperature of gelation.

* Corresponding author.

E-mail address: t.vermonden@uu.nl (T. Vermonden).

Hydrogel systems based on cross-linked CS offer a suitable *in vitro* platform in which encapsulated cells, particularly chondrocytes and mesenchymal stem cells, can survive, proliferate, as well as produce cartilage-like ECM (Guo et al., 2012; Huang et al., 2015; Ingavle, Dormer, Gehrke, & Detamore, 2012; Sawatjui et al., 2015). Moreover, CS is able to confer desirable mechanical properties to implants (Khanlari, Suekama, Detamore, & Gehrke, 2015; Sawatjui, Damrongrungruang, Leeanansaksiri, Jearanaikoon, & Limpaboon, 2014; Zhang et al., 2011). As a result, CS is currently one of the main components of several recently developed hybrid scaffolds studied *in vitro* and *in vivo* (Kuo, Chen, Hsiao, & Chen, 2015; Liao, Qu, Chu, Zhang, & Qian, 2015; Ni et al., 2015; Wei, Wang, Su, Wang, & Qiu, 2015).

The clinical applicability of implantable scaffolds requires hydrogels with a tunable shape and size to match the space of the tissue defect. Moreover, the regenerative potential likely depends on the capacity of the scaffold to mimic the inner structural complexity of tissue. For cartilage regeneration, the possibility to create implants having a multi-layer organization, typical of native tissue is believed to be beneficial, but the feasibility of this approach still represents a challenge (Schoorman et al., 2015). These aspects highlight the need for a sophisticated engineering-based approach that guarantees customized scaffolds with tunable degree of complexity. Bioprinting of hydrogels is an attractive technique to generate 3D scaffolds with reproducible and complex structures. It is based on computer aided deposition of hydrogel filaments in a layer-by-layer fashion (Malda et al., 2013). By changing certain parameters in the 3D printing settings, it is possible to tune the porosity of printed scaffolds. Porosity is an important parameter that can affect cell survival and activity, because porosity provides higher contact area between the implant and the surrounding fluids and, is thus responsible for better oxygen and nutrient supply to encapsulated cells (Malda et al., 2013). The implantation of porous scaffolds may also facilitate cell migration from neighboring tissues that, in turn could offer opportunities to enrich the implant with ECM producing cells (Hunziker & Rosenberg, 1996; Liu, Shu, & Prestwich, 2006). Furthermore, 3D bioprinting offers the opportunity to generate customized hydrogel scaffolds with desired pattern, shape and size.

A 3D printable material needs to have rheological properties allowing its extrusion through a small needle and fast stabilization after deposition to guarantee shape fidelity of the extruded line (Billiet, Vandenhaute, Schelfhout, Van Vlierberghe, & Dubruel, 2012; Malda et al., 2013). This implies that hydrogel materials with shear thinning properties complemented with substantial yield stress behavior are attractive candidates.

In this study, we aimed to design a hydrogel based on UV-cross-linkable CS, *i.e.* methacrylated CS (CSMA) as a candidate biomaterial for cartilage 3D printing. As mentioned before, hydrogels composed of CS and/or other similar polysaccharides display high chondrogenic potential. Nevertheless, they usually lack essential mechanical properties needed for 3D printing applications. Therefore, CSMA was blended with a synthetic thermo-sensitive polymer which has an ABA architecture based on polyethylene glycol (PEG) and partially methacrylated poly(*N*-(2-hydroxypropyl) methacrylamide-mono/dilactate) (pHPMALac), and has already been used for the development of 3D printable hydrogels (Censi et al., 2011). Moreover, hydrogels based on methacrylated pHPMALac-PEG triblock copolymers have been demonstrated to be cytocompatible. In detail, Censi et al. have found an excellent cell survival of embedded equine articular chondrocytes, *i.e.* $94 \pm 3\%$ and $85 \pm 7\%$ after 1 and 3 days of culture, respectively (Censi et al., 2011). For similar hydrogels, adequate cell viability was also found for goat-derived mesenchymal stem cells cultured over a long culture period of 3 weeks (Vermonden et al., 2008). By combining CSMA with a pHPMALac-PEG triblock

copolymer, we aimed to improve the rheological profile, and thus the 3D printing potential of hydrogels based on CSMA, without compromising cytocompatibility. In this scenario, it is evident that the reproducibility of mechanical and 3D printing properties of the hydrogel depends on the reproducibility of the polymers' characteristics, and thus on the robustness of the synthetic procedure used to obtain the polymers (Kirchmayer, Gorkin III, & in het Panhuis, 2015).

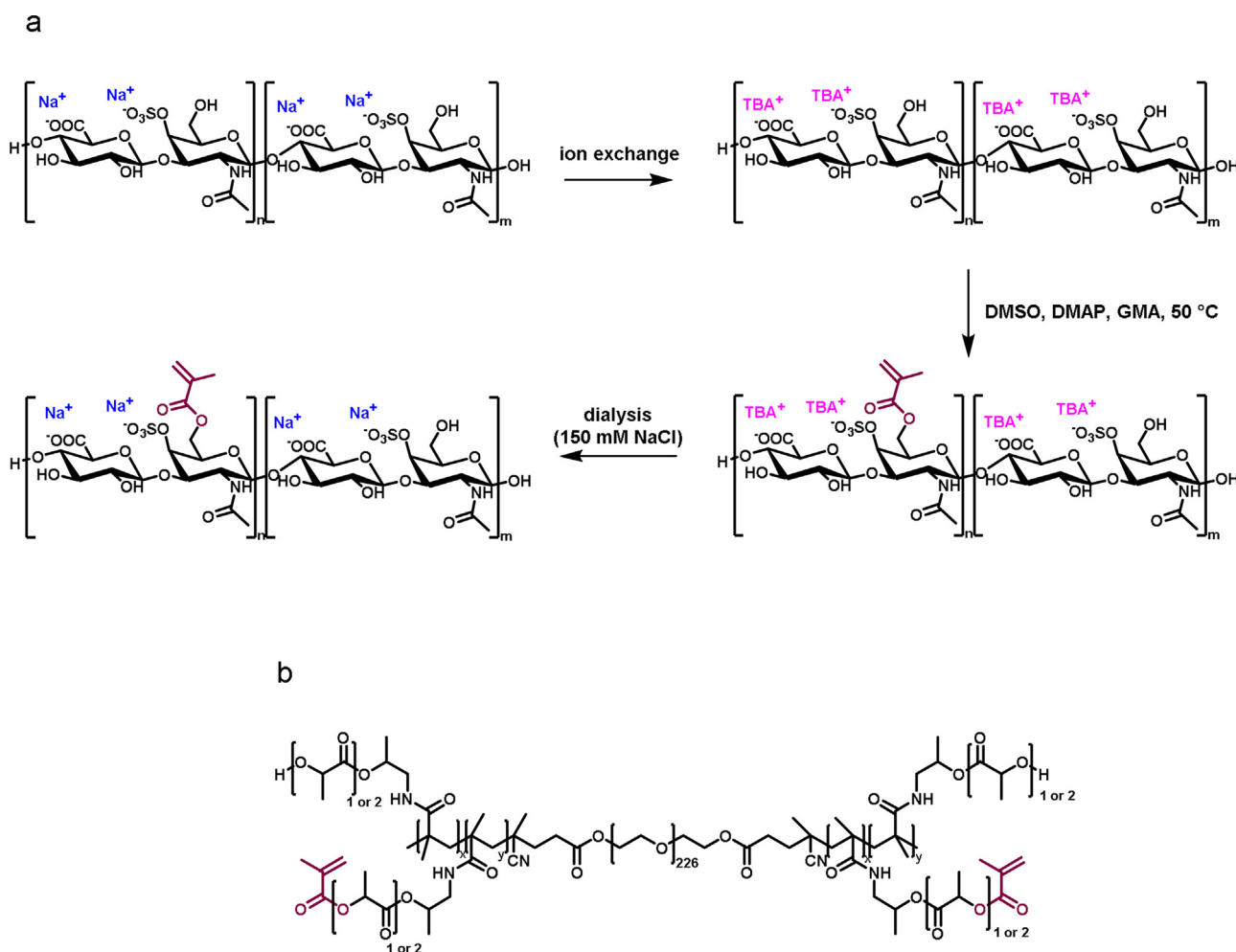
Hence, to obtain CS with a controllable and reproducible degree of methacrylation (DM), we firstly focused on the investigation of an efficient method for the synthesis of CSMA. The two most frequently used methods for methacrylating CS consist of reactions in aqueous solutions using methacrylic anhydride (MA) or glycidyl methacrylate (GMA). When MA is chosen, a large excess of this compound is necessary to compensate for its hydrolysis in water-based medium (Bryant et al., 2004; Guo et al., 2012; Kesti et al., 2015; Steinmetz & Bryant, 2012; Wang, Shen, & Lu, 2003). Moreover, the adjustment of the pH to basic conditions is crucial for the reaction to proceed. The drawback of adding a basic solution to maintain the pH, is that when not accurately dosed this can cause chain scission of the polysaccharide and hydrolysis of the aimed ester bonds after their formation, as was found by Wang and co-workers (Wang et al., 2003). On the other hand, the protocol that employs GMA for the methacrylation of CS in aqueous solution is more efficient (Li, Wang, & Elisseeff, 2003). Nevertheless, it leads to the synthesis of a mixture of products originating from trans-esterification and ring-opening mechanisms, and requires a reaction time of 15 days. Our aim was to develop a GMA trans-esterification procedure, similar as used for the methacrylation of dextran in an aprotic and polar solvent, *i.e.* dimethyl sulfoxide (DMSO) (van Dijk-Wolthuis, Kettenes-van den Bosch, van der Kerk-van Hoof, & Hennink, 1997; van Dijk-Wolthuis et al., 1995), to obtain CS modified with methacrylic functionalities in a fast, efficient, and reproducible manner.

Subsequently, rheological properties of hydrogels composed of CSMA and partially methacrylated pHPMALac-PEG triblock copolymer were compared with those of hydrogels only composed of CSMA or partially methacrylated pHPMALac-PEG triblock. 3D printability of the proposed hydrogel was investigated with the aim to generate 3D printed scaffolds with tunable porosity. Finally, viability and proliferation of chondrogenic cells embedded in the described hydrogel were evaluated.

2. Experimental

2.1. Materials

All chemicals and solvents were obtained from Sigma-Aldrich (Zwijndrecht, the Netherlands) and Biosolve (Valkenswaard, the Netherlands), respectively, unless indicated otherwise. Chemicals and solvents were used as received. Chondroitin sulfate A sodium salt from bovine trachea ($\geq 60\%$ type A (Scheme 1a), balanced with type C), further referred to as CS, was purchased from Sigma-Aldrich. CS was analyzed by Gel Permeation Chromatography (GPC), which showed the presence of three molecular weight distributions. Because of the high polydispersity of the sample, the peak molecular weights (M_p) are reported. The M_p values found for CS were 189 kDa, 13 kDa and 3 kDa, when using dextrans as standards (Fig. S1a). A thermo-sensitive triblock copolymer consisting of a PEG (10000 Da, abbreviated as PEG₁₀₀₀₀) mid-block flanked with two partially methacrylated pHPMALac outer blocks (Scheme 1b) was synthesized and characterized as previously reported (Vermonden et al., 2008). The thermo-sensitive polymer is further referred to as $M_{15}P_{10}$ (M_{15} refers to a degree of methacrylation, DM of 15% and P_{10} refers to a PEG chain length of 10 kDa). Characteristics of $M_{15}P_{10}$ are reported in Table 1. Irgacure 2959



Scheme 1. Reaction scheme for the synthesis of CSMA (a). In the first step Na^+ counter ions are replaced by TBA ions. In the second step methacrylation of the hydroxyl groups of CS occurs. CSMA as sodium salt is obtained after dialysis. Chemical structure of $\text{M}_{15}\text{P}_{10}$ (b). $\text{M}_{15}\text{P}_{10}$ consists of a PEG_{10000} mid-block flanked with two partially methacrylated (DM = 15%) pHPMAlac outer blocks, obtained using a feed molar ratio between (hydroxypropyl) methacrylamide mono- and dilactate of 75:25.

Table 1

Characteristics of $\text{M}_{15}\text{P}_{10}$. Degree of methacrylation (DM), number average molecular weight (Mn), polydispersity index (PDI) and cloud point (CP).

Polymer	DM (%)	Mn (kDa)	PDI	CP ($^{\circ}\text{C}$)
$\text{M}_{15}\text{P}_{10}$	15 ^a	40.6 ^b 34.3 ^c	2.0 ^c	9 ^d

^a Defined as the percentage of hydroxyl groups being methacrylated and determined by ^1H NMR, using DMSO-d_6 as solvent.

^b Determined by ^1H NMR, using DMSO-d_6 as solvent and calculated by comparing the signals of the (hydroxypropyl) methacrylamide lactate protons to those of PEG protons.

^c Determined by GPC, using N,N -dimethylformamide enriched with LiCl (10 mM) as eluent and PEG with narrow MW distributions (Polymer Standards Service, Mainz, Germany) as standards.

^d Determined by UV–vis spectrophotometry and defined as the onset of increasing light scattering during a temperature ramp measurement (4–50 $^{\circ}\text{C}$, 1 $^{\circ}\text{C}/\text{min}$, 650 nm).

was a kind gift from BASF (Ludwigshafen, Germany) and phosphate buffered saline (PBS) was obtained from Braun (Melsungen, Germany). Dulbecco's Modified Eagle Medium: Nutrient Mixture F-12 supplemented with GlutaMax-1 31331 (further referred to as DMEM/F-12), penicillin/streptomycin (pen/strep; 10,000 units/ml penicillin and 10 mg/ml streptomycin) and Click-iT[®] Edu Imaging Kit C10337 proliferation assay, were supplied by Invitrogen (Carlsbad, California, USA). Fetal bovine serum was purchased from Gibco (Invitrogen corporation), whereas recombinant human Fibroblast

Growth Factor-basic (bFGF, 233FB) was supplied by R&D systems (Abingdon, UK).

2.2. Methacrylation of CS

Methacrylation of CS was carried out using a reaction procedure, as reported by Oudshoorn, Rissmann, Bouwstra, and Hennink, (2007) for hyaluronic acid (HA), with some modifications (Scheme 1a). Briefly, Dowex[®] 50WX8 hydrogen form resin (57.5 g) was initially flushed with 225 ml of a water solution containing tetrabutylammonium (TBA) fluoride (61.6 g) and then extensively washed with MilliQ water until the pH of the eluting solution became neutral. As last step, 1.8 l of an aqueous CS solution (10 mg/ml) was eluted through the resin and collected. CS in form of TBA salt (CS-TBA) was recovered after freeze-drying. This product was further analyzed by ^1H -Nuclear Magnetic Resonance (^1H NMR, in DMSO-d_6 , with chemical shifts referred to the solvent residual peak of 2.50 ppm) and the content of TBA per disaccharide unit of CS (ratio TBA:CS) was determined using the following equation:

$$\text{RatioTBA : CS} = \frac{\text{average}(I_{1.57}, I_{1.32})}{8} : \frac{I_{1.77}}{3} \quad (1)$$

To study the kinetics of the methacrylation reaction, 1 g of CS-TBA (1.141 mmol of disaccharide units) was dissolved in 37 ml of DMSO. Next, 4-(N,N -dimethylamino)pyridine (DMAP, 0.1835 g)

Table 2
Polymer solution/hydrogel composition for CSMP₂₊₁₈, CS₂₀ and MP₂₀.

Polymer solution/ hydrogel	CSMA (w/w)	M ₁₅ P ₁₀ (w/w)
CSMP ₂₊₁₈	2%	18%
CS ₂₀	20%	–
MP ₂₀	–	20%

and GMA (155.2 μ l, molar ratio between GMA and CS-TBA disaccharide units = 1:1) were added, and the reaction mixture was stirred under N₂ atmosphere at 50 °C for 3 weeks. At several time-points (45 min, 1.5 h, 3 h, 6 h, 21 h, 29 h, 48 h, 54 h, 76 h, 1 week, 2 weeks, 3 weeks) samples of 3 ml were taken, diluted with 9 ml of water and pH-adjusted to 5.5 using a 0.2 M solution of HCl. The polymer solutions were then dialyzed against NaCl 150 mM solution in water for 3 days and against water for an additional 4 days. Purified CSMA samples for each time point were finally collected, as Na⁺ salt, after freeze-drying. This reaction was performed in triplicate.

To study the effect of the GMA feed on the DM of CSMA, several reactions were carried out: 0.545 g of CS-TBA (0.622 mmol of disaccharide units) was dissolved in 20 ml of dry DMSO under N₂ atmosphere at 50 °C. After addition of DMAP (0.1 g) and GMA (9.0, 19.7, 39.4, 47.3, 59.1, 84.6, 118.3, 185.6 or 263.5 μ l) the reaction mixtures were stirred at 50 °C for 48 h. Subsequently, the mixtures were diluted with 60 ml of water, pH-adjusted to 5.5, dialyzed and freeze-dried as described above.

2.3. Characterization of polysaccharides

CS, CS-TBA and CSMA were characterized by ¹H NMR using a Gemini-300 MHz spectrometer (Varian Associates Inc., NMR Instruments, Palo Alto, CA, USA). D₂O was used as solvent for CS and CSMA, and DMSO-d₆ was used for CS-TBA. Chemical shifts were referred to the solvent residual peak of 4.79 or 2.50 ppm in case of D₂O or DMSO-d₆, respectively. The DM of CSMA, defined as the number of methacrylate groups per 100 disaccharide units, was calculated as follows:

$$DM(\%) = \frac{\text{average}(I_{6.20}, I_{5.77})}{(I_{2.18-1.86} - 3)/3} \times 100 \quad (2)$$

in which the signal at chemical shift 6.20 ppm was normalized for the integration of 1 proton and $I_{2.18-1.86}$ is referred to the region in which the broad signal at chemical shift 2.04 ppm and the signal at chemical shift 1.96 ppm are fully included. CS and CSMA dissolved in D₂O were also characterized by ¹³C NMR. Spectra were recorded during 21 h of scanning using an Agilent 400/54 Premium Shielded NMR Magnet System (Agilent Technologies, Santa Clara, CA, USA). In addition, ¹³C Attached Proton Test (APT) and Distortionless Enhancement by Polarization Transfer (DEPT) spectra were acquired over a scanning period of 10 h. CSMA was also characterized by GPC, using the same method described for CS.

2.4. Rheological measurements

A polymer solution containing 2% w/w of CSMA (DM = 15%) and 18% w/w of M₁₅P₁₀ (DM = 15%) was prepared by dissolving the polymers in phosphate buffered saline pH 7.4 (PBS) under mild stirring overnight at 4 °C and it is further referred to as CSMP₂₊₁₈. Polymer solutions containing only CSMA (20% w/w) or M₁₅P₁₀ (20% w/w) were prepared in the same manner, used as controls and are further referred to as CS₂₀ and MP₂₀, respectively (Table 2).

CSMP₂₊₁₈, CS₂₀ and MP₂₀ were analyzed by a Discovery HR-2 rheometer (TA-Instruments, Etten-Leur, The Netherlands) using a cone-plate measuring geometry (cone diameter: 20 mm, cone angle: 1°, truncation: 27 μ m). To identify the linear viscoelastic region (LVR), samples were subjected to strain sweep experiments

at 37 °C employing a strain range from 0.01 to 100% and a frequency of 1 Hz. The solutions were further analyzed employing a quick temperature ramp (5 °C/min) from 4 to 40 °C in oscillation mode using a strain of 1% and a frequency of 1 Hz. Furthermore, frequency sweep experiments (0.01–100 rad/s) were performed at 37 °C and 1% strain. To investigate possible shear thinning properties, samples were subjected to an increasing shear rate (from 0.006 to 10000 s^{−1}) at 37 °C. Moreover, samples were sheared at 37 °C applying a stress ramp from 0 to 1000 Pa and the shear yield stress (τ_y) was calculated using TA Instruments Trios v3.3.0.4055 software according to the Herschel–Bulkley model (Fu, Saiz, & Tomsia, 2011). Finally, recovery studies (Kesti et al., 2015; Liu & Yao, 2015) were performed at 37 °C in three oscillation steps: first the samples were subjected to a strain of 0.1% for CSMP₂₊₁₈ and MP₂₀, and 1% for CS₂₀ (within the LVR), subsequently a strain of 100% (out of the LVR) was applied and finally a step of 0.1% strain for CSMP₂₊₁₈ and MP₂₀, and 1% strain for CS₂₀ was implemented. The duration of each step was 1 min and the frequency was 1 Hz. A strain of 1% instead of 0.1% was chosen for CS₂₀ because it resulted in a rheogram with higher resolution.

2.5. Swelling behavior of UV cross-linked hydrogels

CSMP₂₊₁₈, CS₂₀ and MP₂₀ polymer solutions prepared as described in Section 2.4 and supplemented with Irgacure 2959 (0.05% w/w) were injected into a teflon mold containing cylindrical wells (diameter: 6 mm, height: 2 mm). Next, the injected polymer solutions were incubated for 5 min at 37 °C to allow physical gelation of CSMP₂₊₁₈ and MP₂₀, and further UV-irradiated for 69 s at 5 cm distance using a Bluepoint 4 UV lamp (point light source, wavelength range: 300–600 nm, intensity at 5 cm: 103 mW/cm², Hönle UV Technology AG, Gräfelfing, Germany). After 3 h of swelling in PBS (pH 7.4), the swelling ratio (SR) of these chemically cross-linked hydrogel discs was calculated as follows:

$$SR = \frac{V_{3h}}{V_{0h}} \quad (3)$$

where V_{3h} and V_{0h} are the measured volumes after 3 h and before swelling, respectively.

To investigate the effect of the DM of CSMA on the final swelling and mechanical properties of hydrogels, discs only composed of CSMA (20% w/w) having different DM, i.e. 7, 20, 27, 35 and 43% were fabricated as described above and the SR was calculated according to equation 3. These hydrogel discs were analyzed for their mechanical properties using a Dynamic Mechanical Analyzer (DMA Q800, TA-Instruments, Etten-Leur, The Netherlands) operating in unconfined compression. Samples were preloaded with a force of 0.001 N, and subsequently compressed using a force ramp rate of 0.1 N/min and an upper force limit of 1 N. The Young's modulus was calculated as the slope of the initial part of the stress/strain curves.

2.6. 3D printing

3D printing of hydrogels was investigated using a 3D Discovery bioprinter platform (RegenHU, Villaz-St-Pierre, Switzerland) equipped with a Bluepoint 4 UV lamp (specifications are given in Section 2.5). The polymer solution was loaded into a dispensing microvalve CF300H print head (needle diameter: 0.3 mm) preheated at 37 °C. The first layer of each construct was generated by dispensing the hydrogel onto glass slides fixed on a baseplate equilibrated at 40 °C. Subsequent layers were obtained by the deposition of alternating horizontal and vertical hydrogel filaments in a bottom-up building fashion. A total of 20 layers for each construct were dispensed and UV-irradiated in a layer-by-layer manner for 3 s. After the deposition of the last layer an additional illumination period of 9 s was used to guarantee a sufficiently stable construct. To

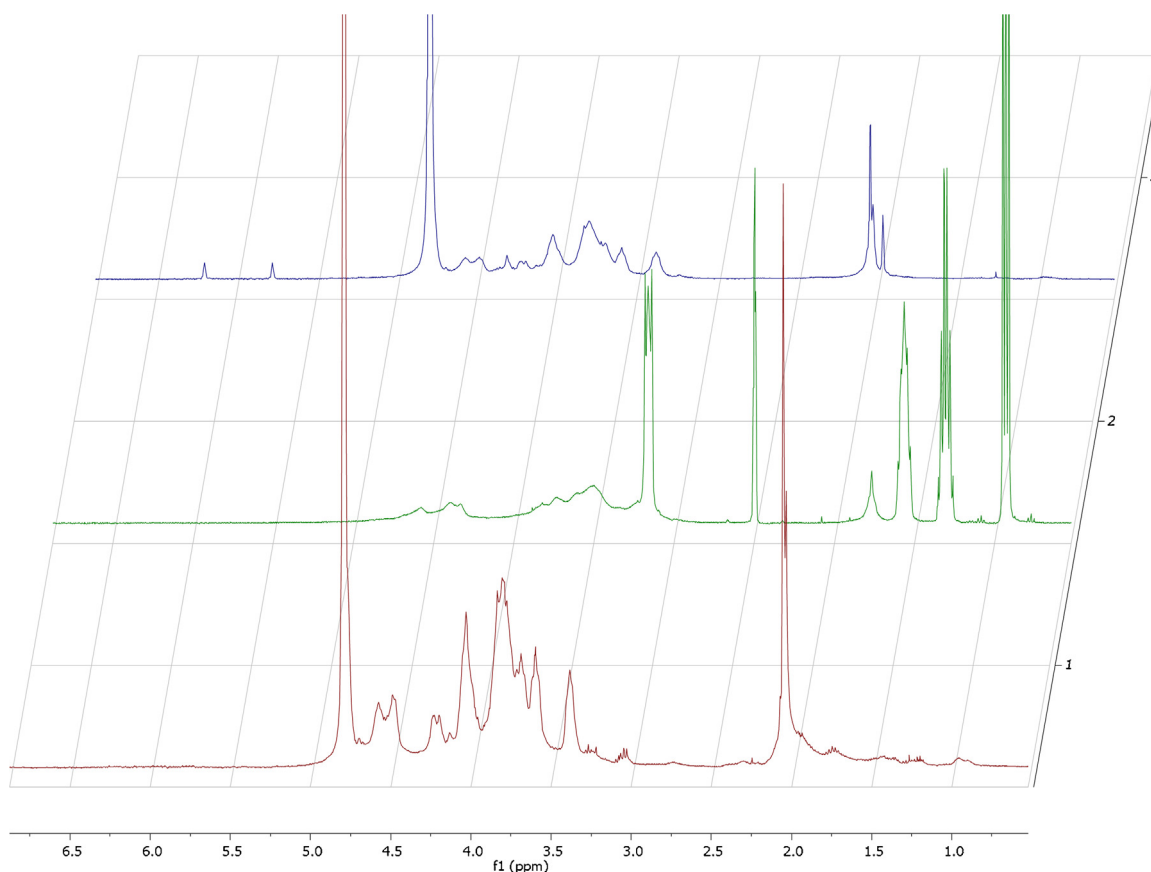


Fig. 1. ^1H NMR spectra of CS (D_2O , bottom spectrum 1, red), CS-TBA ($\text{DMSO}-d_6$, middle spectrum 2, green) and CSMA (D_2O , top spectrum 3, blue). (For interpretation of the references to colour in this figure legend, the reader is referred to the web version of this article.)

generate constructs with different porosity, three line spacing values were used, i.e. 1.25, 1.5 and 2 mm, and the construct dimensions (length and width) were consequently adjusted. Table S1 shows the print-settings used in this study to create 3D porous printed constructs. 3D printed constructs were visualized using an Olympus ZS61 (Tokyo, Japan) microscope fitted with an Olympus (Tokyo, Japan) camera.

2.7. Cell viability and proliferation

To evaluate cellular behavior in the different hydrogels, ATDC5 cells were mixed into the polymer solutions with a final concentration of 7.5×10^6 cells/ml. CSMP₂₊₁₈, MP₂₀ and CS₂₀ cell-laden polymer solutions, containing Irgacure (0.05% w/w) were casted in cylindrical teflon molds as described before (Section 2.5). Constructs were cultured in ATDC5 expansion medium consisting of DMEM/F-12 supplemented with fetal bovine serum (5%), pen/strep (1%) and bFGF (1 ng/ml) for 6 days with a medium change after 3 days of culture. To three samples of each hydrogel formulation, 5-ethynyl-2'-deoxyuridine (EdU) working solution was added at day 1 according to manufacturer's protocol with a final concentration of 5 μM , to be incorporated in the DNA of proliferating cells.

Cell viability was evaluated at day 1, 4 and 6. For all time points, one sample of each formulation was cut in half and stained for 20 min with 4 μM calcein MA (live, Life technologies L3224) and 2 μM ethidium homodimer-1 (dead, Life technologies L3224) in PBS at 37 °C. Samples were washed 3 times for 5 min with PBS and the staining was visualized using an Olympus BX51 microscope. Images were taken at four different locations of each sample at the cross-sectional area for analysis.

To monitor cellular proliferation a Click-iT® EdU assay was performed on samples that were incubated with EdU working solution, according to manufacturer's protocol. In short, at day 6 samples were collected, fixed overnight in formalin (37%), dehydrated via graded ethanol series and xylene, and embedded in paraffin. Tissue sections with a thickness of 5 μm were made and stained for 30 min with the Click-iT reaction cocktail (1x click-iT reaction buffer, CuSO_4 , Alexia Fluor azide, and reaction buffer additive, all provided with the kit) at room temperature to stain the nuclei of proliferated cells green. To stain all cell nuclei blue, samples were incubated for 20 min with 4',6-diamidino-2-phenylindole (DAPI, 0.1 $\mu\text{g}/\text{ml}$) solution at room temperature. Next, samples were visualized with an Olympus BX51 microscope.

2.8. Statistics

Statistical analyses were performed using SPSS software (version 20, IBM Corporation, USA). Differences in viability between groups at each time point were determined with a One-Way ANOVA test with a significance level of 0.05 and a Tukey's Post-hoc analysis. Normality and homogeneity of the data were assumed.

3. Results and discussion

3.1. Synthesis and characterization of CSMA

For the synthesis of CSMA, the Na^+ counter ions were exchanged by the more lipophilic TBA cations to render CS soluble in DMSO. The ^1H NMR spectrum of CS-TBA (Fig. 1, spectrum 2) shows the following signals: δ 5.01–4.26 and 4.12–3.37 (β -glucuronic acid and *N*-acetyl- β -galactosamine-4-sulfate ring

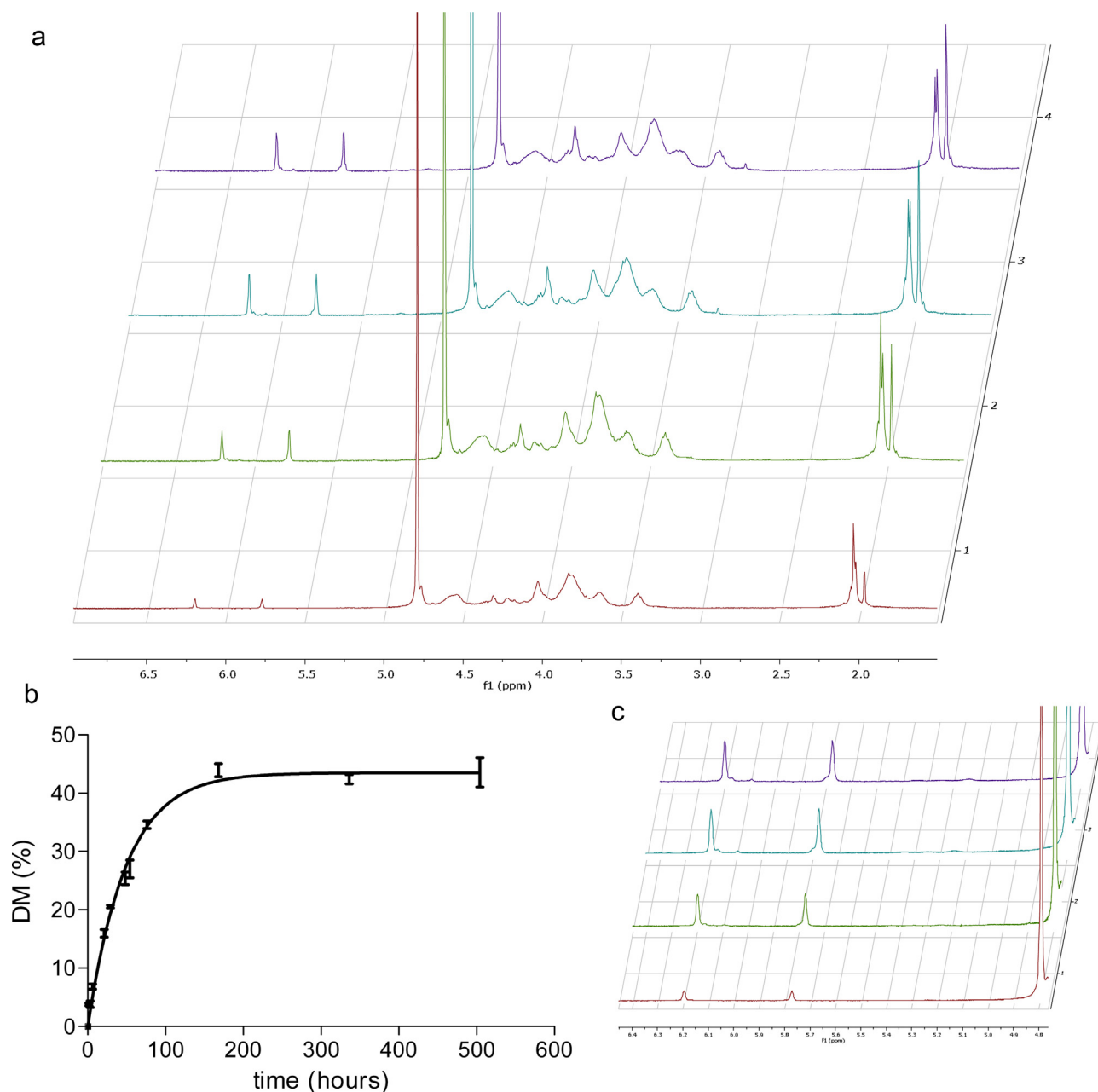


Fig. 2. Kinetic study for the methacrylation of CS. ¹H NMR spectra of CSMA (D₂O) after 21 h (spectrum 1, red), 48 h (spectrum 2, green), 1 week (spectrum 3, blue), and 3 weeks (spectrum 4, purple) (a). DM (%) as a function of time (h) with $n = 3$ (b). Zoom-in of the region between chemical shift 6.4 and 4.8 ppm of the ¹H NMR spectra reported in Fig. 2a (c). (For interpretation of the references to colour in this figure legend, the reader is referred to the web version of this article.)

protons), δ 3.16 (8H for each TBA unit, $\text{N}^+(\text{CH}_2(\text{CH}_2)_2\text{CH}_3)_4$), δ 1.77 (3H for each disaccharide unit, CH_3CONH), δ 1.57 (8H for each TBA unit, $\text{N}^+(\text{CH}_2\text{CH}_2\text{CH}_2\text{CH}_3)_4$), δ 1.32 (8H for each TBA unit, $\text{N}^+((\text{CH}_2)_2\text{CH}_2\text{CH}_3)_4$), δ 0.93 (12H for each TBA unit, $\text{N}^+((\text{CH}_2)_3\text{CH}_3)_4$). The appearance of the signals corresponding to the protons present in the four aliphatic chains of TBA, confirmed that the ion exchange occurred, and showed that almost each disaccharide unit of CS contained two TBA moieties (ratio TBA:CS = 1.73). Subsequently, a partial esterification of the hydroxyl groups on CS-TBA was performed in DMSO using GMA as methacrylating agent to obtain CSMA. For CSMA, the following signals were observed: δ 6.20 and 5.77 (2H for each methacrylate group, $\text{CH}_2=\text{C}(\text{CH}_3)$), δ 4.71–3.10 (β -glucuronic acid and *N*-acetyl- β -galactosamine-4-sulfate ring protons), δ 2.04 (3H for each disaccharide unit, CH_3CONH), δ 1.96 (3H for each methacrylate group, $\text{CH}_2=\text{C}(\text{CH}_3)$) (Fig. 1, spec-

trum 3). The presence of the signals at chemical shifts 6.20, 5.77 and 1.96 ppm, attributed to the protons present in the methacrylate group, proved that methacrylation occurred. Moreover, the efficient removal of the organic cation after methacrylation and dialysis was confirmed by the disappearance of the above mentioned signals of the TBA protons at 3.16, 1.57, 1.32 and 0.93 ppm (Fig. 1, spectrum 3).

The study on the reaction kinetics was performed using a fixed GMA:CS-TBA disaccharide unit feed ratio of 1:1 and was carried out for 3 weeks. The first time point at which methacrylation of CS was detectable in the ¹H NMR spectrum was after 1.5 h, where a DM of 4% was found. In Fig. 2a, ¹H NMR spectra of CSMA recovered after a reaction time of 21 h, 48 h, 1 week and 3 weeks are reported. In the first three spectra, an increase of the signals at 6.20 and 5.77 ppm, representative of the vinyl protons of the

methacrylate groups was observed together with a related increase of the signal at 1.96 ppm, representative of the methyl group of the methacrylate functionality. In general, the DM increased by increasing the reaction time for the first 7 days, after which it leveled off at $43 \pm 1\%$ (Fig. 2b). This plateau is likely attributed to an equilibrium-state dictated by the increasing amount of glycidol formed, responsible for competing nucleophilic attack on GMA molecules and/or on CSMA (Oudshoorn, Rissmann, Bouwstra, & Hennink, 2006; van Dijk-Wolthuis, Kettenes-van den Bosch et al., 1997). From this study, it was calculated that the minimal unincorporated GMA was approximately 57%. Based on this observation, the methacrylation of CS under these conditions seems to proceed less efficiently than the methacrylation of dextran, where more than 90% of the added GMA was incorporated under optimized conditions (van Dijk-Wolthuis et al., 1995). This might be attributed to the steric hindrance due to the presence of the TBA ions and/or sulfate groups in CS-TBA and/or to the more diluted conditions used for the methacrylation of CS. Nevertheless, to the best of our knowledge, the reaction efficiency found in our study is considerably higher than any other previously reported methods for the methacrylation of CS. More importantly, the methacrylation reaction described herein is highly reproducible, as shown by the low standard deviation found for the DM values reported in Fig. 2b.

Another important aspect was to determine whether the described reaction proceeded via ring-opening or transesterification or via both mechanisms. When CS was firstly methacrylated in aqueous conditions using GMA by Li and collaborators, the presence of CS derivatives produced by ring-opening was proven by the appearance of signals at 5.5 and 5.2 ppm in the ^1H NMR spectra, representative of the CH protons on the glyceryl spacer generated by reaction of the sulfate group or the carboxyl group of CS with the epoxide ring of GMA (Li et al., 2003). In contrast, as can be seen in the ^1H NMR spectra of CSMA synthesized according to our method (Fig. 2c), even after 3 weeks of reaction, there is no sign of the above mentioned signals. Hence, ring-opening does not occur under the reaction conditions we used and this observation is in line with the findings reported for the methacrylation of dextran and hyperbranched polyglycerol with GMA in DMSO (Oudshoorn et al., 2006; van Dijk-Wolthuis, Kettenes-van den Bosch et al., 1997).

To investigate the position of the methacrylate groups in CSMA, ^{13}C NMR spectra of CS and CSMA after 48 h of reaction, in combination with APT and DEPT spectra were used (Fig. S2a–f). These analyses showed that the methacrylation of CS after 48 h of reaction occurs on both primary and secondary OH groups of CS. Nevertheless, considering the integrations of the ^{13}C NMR signals, we could observe, as expected that a slightly preferential substitution of primary OH took place.

Several reactions employing different amounts of GMA were used to identify the dependence of the DM on the GMA feed. Fig. 3 shows the obtained DM (%) as a function of the feed molar ratio between GMA and the disaccharide units of CS-TBA. As expected, DM increased with increasing GMA feed and a typical variation of $\sim 6\%$ was found. Finally, GPC analysis on native CS and CSMA (Fig. S1b and c) confirmed that no chain scission occurred during the reaction.

The opportunity to accurately tailor the DM of poly-alcohols via transesterification from GMA is well known in literature and it was extensively applied to dextran (Chiu, Lin, & Hsu, 2002; Gu et al., 2009; van Dijk-Wolthuis et al., 1995; van Dijk-Wolthuis, Hoogetboom et al., 1997; van Dijk-Wolthuis, Kettenes-van den Bosch et al., 1997; van Dijk-Wolthuis, van Steenberg et al., 1997) as well as to polyglycerol (Oudshoorn et al., 2006; Oudshoorn, Penterman et al., 2007), and to a lesser extent also to HA (Oudshoorn, Rissmann et al., 2007). To the best of our knowledge, it has not been reported for CS, while this method combines a high

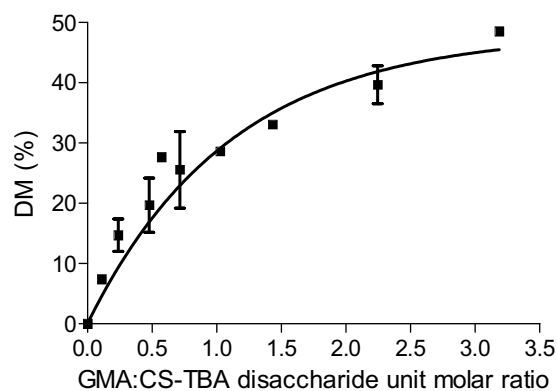


Fig. 3. DM (%) as a function of GMA:CS-TBA disaccharide unit molar ratio.

efficiency due to water free reaction conditions with a reaction robustness that in turn leads to reproducible tuning of the DM. In summary, the synthesis procedure employed here makes use of an organic solvent, *i.e.* DMSO under water-free conditions, which allows for a highly controlled, reproducible and efficient methacrylation of CS.

3.2. Rheological properties of polymer solutions

Oscillatory temperature ramp experiments were performed within the linear viscoelastic region (LVR), which was identified by means of strain sweep experiments (Fig. S3a). For CSMP₂₊₁₈ it was found that G' increases by raising the temperature from 4 to 40 °C (Fig. 4a). The storage modulus (G') at 40 °C was 380.8 ± 2.5 Pa, whereas the temperature at which G' crosses the loss modulus (G'') was 21.4 °C and this is here referred to as temperature of gelation (T_{gel}). In line with previously reported studies (Censi et al., 2011; Vermonden et al., 2010), similar behavior was also found for MP₂₀. However, a lower G' at 40 °C (248.1 ± 0.9 Pa) and a remarkably higher T_{gel} (37.8 °C) were found for MP₂₀ in comparison to CSMP₂₊₁₈. These findings confirm the thermo-responsive character of MP₂₀ and CSMP₂₊₁₈. In both cases the physical hydrogel formation is imputable to the self-assembly of M₁₅P₁₀ in aqueous medium at elevated temperatures. In fact, pHPMALac-PEG triblock copolymers and their methacrylated derivatives are known as amphiphilic polymers characterized by a temperature-dependent solubility in water (Vermonden et al., 2008; Vermonden, Besseling, van Steenberg, & Hennink, 2006). In detail, at sufficiently high temperature, the thermodynamically preferred organization consists of self-assembled polymer chains due to dehydration of the outer blocks of the polymer. Hence, for a certain range of concentrations this phenomenon is responsible for physical gel formation. Importantly, CSMA at the tested concentration does not prevent the temperature-dependent self-assembly of M₁₅P₁₀ and clearly participates in the formation of more stiff physical gels compared with the gels only composed of M₁₅P₁₀. In line with expectations, CS₂₀ did not show any thermo-responsivity, since almost constantly low values of G' and G'' (also with $G'' > G'$) were found indicating liquid-like behavior during the entire temperature ramp.

A general increase of G' and G'' was visible when CSMP₂₊₁₈, MP₂₀ and CS₂₀ samples were sheared at increasing frequency. Nevertheless, only for CSMP₂₊₁₈, G' was continuously higher than G'' at 37 °C and $\tan \delta$ (G''/G') was constant (0.56 ± 0.02) over a wide frequency range, indicating critical gel behavior (Fig. S3b) (Vermonden et al., 2006).

A shear rate test was performed on CSMP₂₊₁₈ to investigate the material's response under high shear rate and, hence the suitability of this material as a potential bioink. Ideally, a printable hydrogel should decrease its viscosity at the shear forces (approximate shear

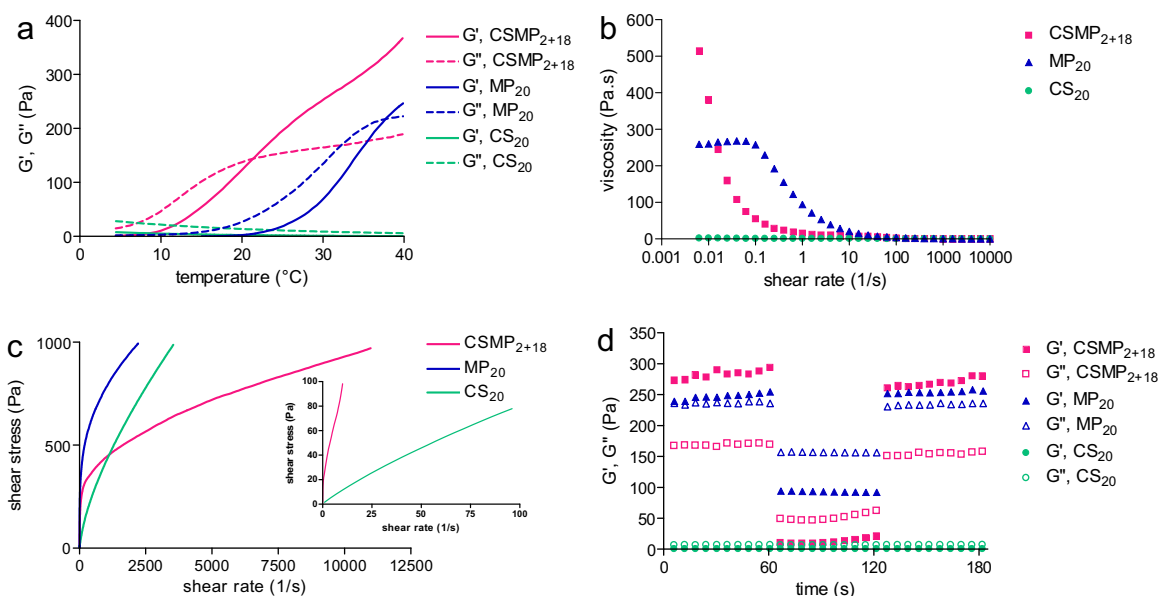


Fig. 4. Rheological properties of CSMP₂₊₁₈, MP₂₀ and CS₂₀. G' and G'' as function of temperature for CSMP₂₊₁₈, MP₂₀ and CS₂₀, recorded during a temperature ramp (4–40 °C, 5 °C/min) using a strain value of 1% and a frequency of 1 Hz (a). Viscosity as a function of shear rate for CSMP₂₊₁₈, MP₂₀ and CS₂₀, recorded during a shear rate sweep (0.006–10000 s⁻¹) at 37 °C (b). Shear stress as a function of shear rate for CSMP₂₊₁₈, MP₂₀ and CS₂₀, recorded during a stress ramp (0–1000 Pa) at 37 °C. In the insert, zoomed-in view at low shear rate for CSMP₂₊₁₈ and CS₂₀ (c). G' and G'' as function of three time-steps where strain was applied at 37 °C in a low-high-low (0.1 or 1%–100%–0.1 or 1%) fashion to CSMP₂₊₁₈, MP₂₀ and CS₂₀, using a frequency of 1 Hz (d). (For interpretation of the references to colour in this figure legend, the reader is referred to the web version of this article.)

rate, $\dot{\gamma} = 100\text{--}500\text{ s}^{-1}$) acting on it in the syringe of a printer to be able to flow through the needle (Malda et al., 2013). Fig. 4b shows that the viscosity of CSMP₂₊₁₈ hydrogel decreased from 514 Pa·s ($\dot{\gamma} = 0.006\text{ s}^{-1}$) to 0.1 Pa·s ($\dot{\gamma} = 10000\text{ s}^{-1}$), which demonstrates that this hydrogel displays clear shear-thinning behavior. This feature can be ascribed to the temporarily destruction of the physical interactions and alignment of the polymer chains in the flow direction under high shear rate. On the other hand, MP₂₀ showed less pronounced shear thinning properties (decrease in viscosity from 259 to 0.2 Pa·s) and CS₂₀ was characterized by a low viscosity independent of the applied shear rate, suggesting liquid Newtonian behavior not suitable for 3D printing applications.

In Fig. 4c shear stress/rate curves are reported. Fitting the curves of both control formulations MP₂₀ and CS₂₀ to the Herschel–Bulkley model, no yield stress (τ_y) was found. In contrast, for CSMP₂₊₁₈ a τ_y of 19.2 ± 7.0 Pa was found (Fig. 4c, insert), with a typical R^2 value of 0.99. Having a yield point is a crucial requirement for a printable hydrogel and defines the stress above which the hydrogel starts to flow and below which it maintains its shape (Malda et al., 2013).

When recovery tests (Fig. 4d) were implemented on CSMP₂₊₁₈, a constant G' of 283 ± 7 Pa was found at low strain (0.1%) deformation. In the subsequent step, during which a high strain (100%) was applied, an immediate drop of G' to 10.8 Pa was measured, while in the final step when low strain was applied, the initial G' value was rapidly restored. This test indicates that the physical polymer network existing at low strain at 37 °C is efficiently and quickly broken at high strain as proven by G'' values significantly higher than G' during the second step of the measurement. Moreover, the return of high G' values, rapidly after lowering the strain is a sign of quick recovery of the physical polymer network. This rapid recovery is a crucial requirement in 3D printing, since it guarantees the good shape fidelity of the hydrogel filament after extrusion.

To summarize, CSMP₂₊₁₈ is a thermo-sensitive hydrogel able to form a physically cross-linked polymer network by raising the temperature. It is a critical gel, capable to shear-thin under sufficiently high shear rate and able to quickly recover its initial structure after deformation, thanks to its yield stress behavior.

3.3. Swelling behavior of UV cross-linked hydrogels

Chemically cross-linked hydrogel discs were obtained using a casting procedure based on injection molding and UV light exposure as described in Section 2.5. Fig. 5a shows the SR of CSMP₂₊₁₈, MP₂₀ and CS₂₀ hydrogels. The SR found for CS₂₀ ($\text{SR} = 2.06 \pm 0.02$) was higher than the SR of CSMP₂₊₁₈ ($\text{SR} = 1.34 \pm 0.03$) and MP₂₀ (1.37 ± 0.04). The difference in swelling between CSMP₂₊₁₈ and CS₂₀ is also visible from the photographs reported in Fig. 5b and c. This phenomenon is likely attributed to the higher CSMA content in CS₂₀ hydrogels, which is a hydrophilic charged polymer responsible for a large water uptake (Lee, Kung, & Lee, 2005; Varghese et al., 2008). Ideally, minimal swelling behavior is often desired for implantable hydrogels to guarantee their stability at the implantation site (Hayami, Waldman, & Amsden, 2015) and to maintain the initial shape of printed constructs. Therefore, the lower swelling of CSMP₂₊₁₈ hydrogels compared with CS₂₀ hydrogels is a relevant feature. Interestingly, the turbidity of CSMP₂₊₁₈ hydrogels suggests that these hydrogels are phase-separated systems. Blending the PEG-containing amphiphilic M₁₅P₁₀ with the hydrophilic CSMA at the reported concentrations and temperature seems to lead to the formation of an aqueous polymer/polymer two phase system likely similar to that described for PEG and dextran (Albertsson, 1958).

Finally, swelling and mechanical studies carried out on hydrogels only composed of CSMA with different DM, showed that the SR of these hydrogels decreased from approximately 4 to 2 by increasing the DM from 7 to 43% (Fig. S4). This trend can be explained by the fact that a higher DM of CSMA is responsible for lower polymer hydrophilicity, and more importantly for a higher cross-linking density of the polymer network, which leads to a decreased water uptake. In line with expectations, the Young's modulus increased from 7.9 ± 0.8 kPa to 59.8 ± 3.0 kPa by increasing the DM from 7 to 27%. The absence of a further increase of the Young's modulus for DM higher than 27% can likely be ascribed to a less efficient conversion of the methacrylate groups due to restricted mobility of highly methacrylated CS chains (Hachet, Van Den Berghe, Bayma, Block, & Auzély-Velty, 2012).

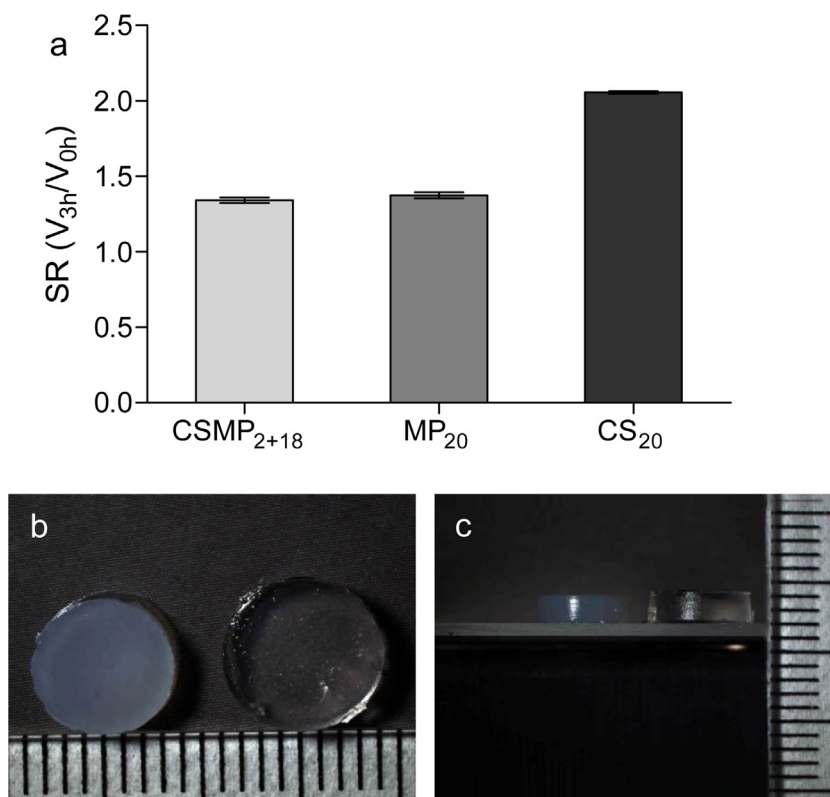


Fig. 5. Swelling ratios (SR) for CSMP₂₊₁₈, MP₂₀ and CS₂₀ hydrogels (a). Photographs of discs composed of CSMP₂₊₁₈ (left) and CS₂₀ (right) from a top view (b) and a side view (c).

3.4. 3D printing of hydrogel

3D printing of CSMP₂₊₁₈ under optimized conditions (Table S1) resulted in the deposition of well-defined hydrogel filaments and led to the generation of 3D porous constructs. In Fig. 6, photographs of constructs in swollen state, having line spacing of 1.25, 1.5 and 2 mm, respectively are shown. From these top-viewed pictures, a defined vertical porosity can be appreciated. It needs to be noted that the flexibility of the constructs under handling increased by decreasing the mesh size. For the construct having the widest strand spacing, *i.e.* 2 mm, the flexibility of the cross-linked filaments under handling was higher compared with the other two construct designs. For this reason the pores in the 2 mm strand-spaced construct appear less homogeneously shaped. Nevertheless, all the generated constructs were successfully handled with a spatula without damage. A side view of one of the printed constructs is reported in Fig. S5, where it can be observed that the aimed height of 2 mm was accurately achieved.

To summarize, the suitability of CSMP₂₊₁₈ as a 3D printable material is in line with the rheological properties described in Section 3.2 and a proper 3D printing principle can be described for this hydrogel. In detail, CSMP₂₊₁₈ is in a physically cross-linked state when loaded into the cartridge of the printer; subsequently, when a pressure is applied, shear forces cause the temporary disruption of the network and allow the flow of the gel through the needle of the printer. Next, the quick recovery of the physical structure after extrusion, driven by zero-shear rate and high temperature at the deposition site, is responsible for the good shape fidelity of each filament.

3.5. Cell viability and proliferation

ATDC5 cells were incorporated in the different hydrogel formulations. At day 1 of culture, $94 \pm 5\%$ of the cells encapsulated

in formulation CSMP₂₊₁₈ were viable, while significantly less living cells were observed in MP₂₀ gels ($80 \pm 3\%$, Fig. 7). In CS₂₀ gels, $99 \pm 1\%$ of the embedded cells were viable at day 1. After 4 days of culture, cell viability decreased in the CSMP₂₊₁₈ group to $66 \pm 10\%$, which was significantly lower compared to MP₂₀ and CS₂₀ gels ($93 \pm 1\%$ and $94 \pm 4\%$, respectively) at this time point. After 6 days of culture no significant differences were present between the groups and $78 \pm 20\%$, $92 \pm 2\%$, and $98 \pm 2\%$ of the cells were alive in CSMP₂₊₁₈, MP₂₀ and CS₂₀, respectively. Additionally, a typical round morphology of ATDC5 cells was observed for all hydrogels at each time point.

To investigate cellular proliferation, samples were cultured with EdU. Multiple EdU positive cells were detected in CSMP₂₊₁₈ hydrogels, indicating that even though some cells died during the first days of culture, the remaining cells were viable and capable of proliferating (Fig. 7, EdU staining results of MP₂₀ and CS₂₀ hydrogels are shown in Fig. S6). Taken together, CSMP₂₊₁₈ hydrogels are suitable materials for cell encapsulation showing adequate cell viability and proliferation of ATDC5 cells over a culture period of at least 6 days.

4. Conclusions

In this work, a novel method for the methacrylation of CS is described and it allows for a tailorable and controllable DM. The reaction proceeds via trans-esterification mechanism and results in the substitution of both primary and secondary hydroxyl groups of CS. Hydrogels based on CSMA and thermo-sensitive M₁₅P₁₀ have been investigated for their rheological properties and revealed their superiority over hydrogels only composed of CSMA or M₁₅P₁₀. Unlike the control formulations, CSMP₂₊₁₈ showed strain-softening, thermo-sensitive and shear thinning behavior combined with yield stress properties. These characteristics render CSMP₂₊₁₈ hydrogel suitable for the 3D printing of TE implants. In fact, it was successfully used as a hydrogel-based ink to gener-

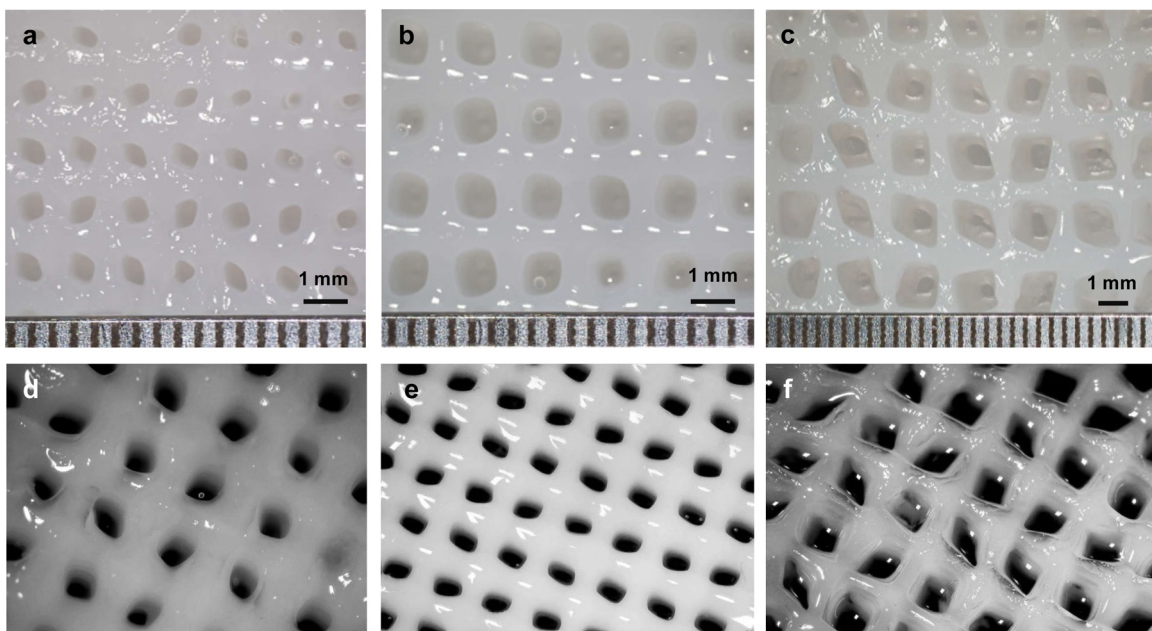


Fig. 6. Photographs of 3D printed constructs. Top view of constructs printed using a strand spacing of 1.25 mm (a), 1.5 mm (b), and 2 mm (c). Skewed top view of 3D printed constructs having a strand spacing of 1.25 mm (d), 1.5 mm (e), and 2 mm (f).

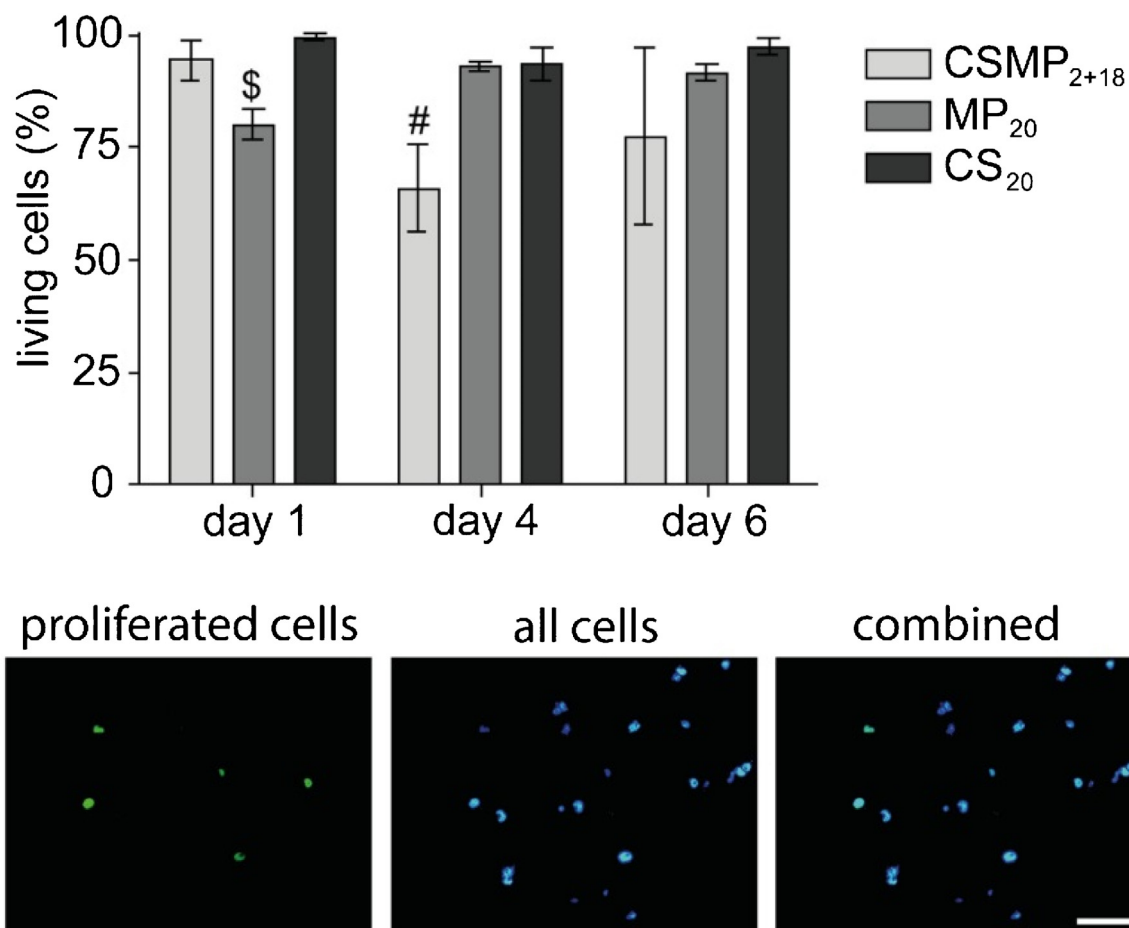


Fig. 7. Viability of ATDC5 cells embedded in CSMP₂₊₁₈, MP₂₀ and CS₂₀ hydrogels. Percentage of living cells after 1, 4 and 6 days of culture, where \$ and # indicate that the group is significantly lower than the other two groups at the same time point (\$ $p = 0.000$; # $p = 0.000$) (top). Proliferated cells (left image, green staining), all cells (middle image, blue staining) and combined pictures (right image) after 6 days of culture for CSMP₂₊₁₈ hydrogels (bottom). Scale bar represents 50 μm. (For interpretation of the references to colour in this figure legend, the reader is referred to the web version of this article.)

ate photo-polymerized 3D constructs with tunable porosity. The 3D printability and the opportunity to tailor the porosity of manufactured constructs confer a versatile character to this hydrogel system. Moreover, adequate survival and proliferation were found for chondrogenic cells embedded in this hydrogel. Taken together, the combination of CSMA and a synthetic PMPALac-PEG triblock copolymer allowed the design of hydrogels where a cell-friendly environment and desirable mechanical characteristics are warranted.

Acknowledgement

The research leading to these results has received funding from the European Union's Seventh Framework Programme (FP7/2007–2013) under grant agreement number 309962 (project HydroZONES).

Appendix A. Supplementary data

Supplementary data associated with this article can be found, in the online version, at <http://dx.doi.org/10.1016/j.carbpol.2016.04.080>.

References

- Albertsson, P.-Å. (1958). Particle fractionation in liquid two-phase systems. The composition of some phase systems and the behaviour of some model particles in them. Application to the isolation of cell walls from microorganisms. *Biochimica et Biophysica Acta*, 27, 378–395. [http://dx.doi.org/10.1016/0006-3002\(58\)90345-7](http://dx.doi.org/10.1016/0006-3002(58)90345-7)
- Billiet, T., Vandenhaute, M., Schelfhout, J., Van Vlierberghe, S., & Dubruel, P. (2012). A review of trends and limitations in hydrogel-rapid prototyping for tissue engineering. *Biomaterials*, 33(26), 6020–6041. <http://dx.doi.org/10.1016/j.biomaterials.2012.04.050>
- Bryant, S. J., Davis-Arehart, K. A., Luo, N., Shoemaker, R. K., Arthur, J. A., & Anseth, K. S. (2004). Synthesis and characterization of photopolymerized multifunctional hydrogels: water-soluble poly(vinyl alcohol) and chondroitin sulfate macromers for chondrocyte encapsulation. *Macromolecules*, 37(18), 6726–6733. <http://dx.doi.org/10.1021/ma0499324>
- Censi, R., Schuurman, W., Malda, J., di Dato, G., Burgisser, P. E., Dhert, W. J. A., & Hennink, W. E. (2011). A printable photopolymerizable thermosensitive p(HPMAm-lactate)-PEG hydrogel for tissue engineering. *Advanced Functional Materials*, 21(10), 1833–1842. <http://dx.doi.org/10.1002/adfm.201002428>
- Chiu, H.-C., Lin, Y.-F., & Hsu, Y.-H. (2002). Effects of acrylic acid on preparation and swelling properties of pH-sensitive dextran hydrogels. *Biomaterials*, 23(4), 1103–1112. [http://dx.doi.org/10.1016/S0142-9612\(01\)00222-8](http://dx.doi.org/10.1016/S0142-9612(01)00222-8)
- Chung, C., Beecham, M., Mauck, R. L., & Burdick, J. A. (2009). The influence of degradation characteristics of hyaluronic acid hydrogels on in vitro neocartilage formation by mesenchymal stem cells. *Biomaterials*, 30(26), 4287–4296. <http://dx.doi.org/10.1016/j.biomaterials.2009.04.040>
- Erickson, I. E., Huang, A. H., Sengupta, S., Kestle, S., Burdick, J. A., & Mauck, R. L. (2009). Macromer density influences mesenchymal stem cell chondrogenesis and maturation in photocrosslinked hyaluronic acid hydrogels. *Osteoarthritis and Cartilage*, 17(12), 1639–1648. <http://dx.doi.org/10.1016/j.joca.2009.07.003>
- Fu, Q., Saiz, E., & Tomsia, A. P. (2011). Direct ink writing of highly porous and strong glass scaffolds for load-bearing bone defects repair and regeneration. *Acta Biomaterialia*, 7(10), 3547–3554. <http://dx.doi.org/10.1016/j.actbio.2011.06.030>
- Gu, C., Zheng, R., Yang, Z., Wen, A., Wu, H., Zhang, H., & Yi, D. (2009). Novel glycidyl methacrylated dextran/gelatin nanoparticles loaded with basic fibroblast growth factor: formulation and characteristics. *Drug Development and Industrial Pharmacy*, 35(12), 1419–1429. <http://dx.doi.org/10.3109/03639040902988558>
- Guo, Y., Yuan, T., Xiao, Z., Tang, P., Xiao, Y., Fan, Y., & Zhang, X. (2012). Hydrogels of collagen/chondroitin sulfate/hyaluronan interpenetrating polymer network for cartilage tissue engineering. *Journal of Materials Science: Materials in Medicine*, 23(9), 2267–2279. <http://dx.doi.org/10.1007/s10856-012-4684-5>
- Hachet, E., Van Den Bergh, H., Bayma, E., Block, M. R., & Auzély-Velty, R. (2012). Design of biomimetic cell-interactive substrates using hyaluronic acid hydrogels with tunable mechanical properties. *Biomacromolecules*, 13(6), 1818–1827. <http://dx.doi.org/10.1021/bm300324m>
- Hayami, J. W. S., Waldman, S. D., & Amsden, B. G. (2015). Photo-cross-linked methacrylated polysaccharide solution blends with high chondrocyte viability, minimal swelling, and moduli similar to load bearing soft tissues. *European Polymer Journal*, 72, 687–697. <http://dx.doi.org/10.1016/j.eurpolymj.2015.01.038>
- Hu, X., Li, D., Zhou, F., & Gao, C. (2011). Biological hydrogel synthesized from hyaluronic acid, gelatin and chondroitin sulfate by click chemistry. *Acta Biomaterialia*, 7(4), 1618–1626. <http://dx.doi.org/10.1016/j.actbio.2010.12.005>
- Huang, Z., Nooeaid, P., Kohl, B., Roether, J. A., Schubert, D. W., Meier, C., & Schulze-Tanzil, G. (2015). Chondrogenesis of human bone marrow mesenchymal stromal cells in highly porous alginate-foams supplemented with chondroitin sulfate. *Materials Science and Engineering: C*, 50, 160–172. <http://dx.doi.org/10.1016/j.msec.2015.01.082>
- Hunziker, E. B., & Rosenberg, L. C. (1996). Repair of partial-thickness defects in articular cartilage: cell recruitment from the synovial membrane. *The Journal of Bone and Joint Surgery. American Volume*, 78(5), 721–733.
- Ingavle, G. C., Dormer, N. H., Gehrke, S. H., & Detamore, M. S. (2012). Using chondroitin sulfate to improve the viability and biosynthesis of chondrocytes encapsulated in interpenetrating network (IPN) hydrogels of agarose and poly(ethylene glycol) diacrylate. *Journal of Materials Science: Materials in Medicine*, 23(1), 157–170. <http://dx.doi.org/10.1007/s10856-011-4499-9>
- Kesti, M., Müller, M., Becher, J., Schnabelrauch, M., D'Este, M., Eglin, D., & Zenobi-Wong, M. (2015). A versatile bioink for three-dimensional printing of cellular scaffolds based on thermally and photo-triggered tandem gelation. *Acta Biomaterialia*, 11, 162–172. <http://dx.doi.org/10.1016/j.actbio.2014.09.033>
- Khanlari, A., Suekama, T. C., Detamore, M. S., & Gehrke, S. H. (2015). Structurally diverse and readily tunable photocrosslinked chondroitin sulfate based copolymers. *Journal of Polymer Science Part B: Polymer Physics*, 53(15), 1070–1079. <http://dx.doi.org/10.1002/polb.23751>
- Kirchmayer, D. M., Gorkin, R., III, & in het Panhuis, M. (2015). An overview of the suitability of hydrogel-forming polymers for extrusion-based 3D-printing. *Journal of Materials Chemistry B*, 3(20), 4105–4117. <http://dx.doi.org/10.1039/C5TB00393H>
- Ko, C.-S., Huang, J.-P., Huang, C.-W., & Chu, I.-M. (2009). Type II collagen-chondroitin sulfate-hyaluronan scaffold cross-linked by genipin for cartilage tissue engineering. *Journal of Bioscience and Bioengineering*, 107(2), 177–182. <http://dx.doi.org/10.1016/j.jbiosc.2008.09.020>
- Kuo, C.-Y., Chen, C.-H., Hsiao, C.-Y., & Chen, J.-P. (2015). Incorporation of chitosan in biomimetic gelatin/chondroitin-6-sulfate/hyaluronan cryogel for cartilage tissue engineering. *Carbohydrate Polymers*, 117, 722–730. <http://dx.doi.org/10.1016/j.carbpol.2014.10.056>
- Lee, C.-T., Kung, P.-H., & Lee, Y.-D. (2005). Preparation of poly(vinyl alcohol)-chondroitin sulfate hydrogel as matrices in tissue engineering. *Carbohydrate Polymers*, 61(3), 348–354. <http://dx.doi.org/10.1016/j.carbpol.2005.06.018>
- Levet, P. A., Melchels, F. P. W., Schrobback, K., Huttmacher, D. W., Malda, J., & Klein, T. J. (2014). A biomimetic extracellular matrix for cartilage tissue engineering centered on photocurable gelatin, hyaluronic acid and chondroitin sulfate. *Acta Biomaterialia*, 10(1), 214–223. <http://dx.doi.org/10.1016/j.actbio.2013.10.005>
- Li, Q., Wang, D., & Elisseff, J. H. (2003). Heterogeneous-phase reaction of glycidyl methacrylate and chondroitin sulfate: mechanism of ring-opening-transesterification competition. *Macromolecules*, 36(7), 2556–2562. <http://dx.doi.org/10.1021/ma021190w>
- Liao, J., Qu, Y., Chu, B., Zhang, X., & Qian, Z. (2015). Biodegradable CSMA/PECA/graphene porous hybrid scaffold for cartilage tissue engineering. *Scientific Reports*, 5, 9879. <http://dx.doi.org/10.1038/srep09879>
- Liu, Y., Shu, X. Z., & Prestwich, G. D. (2006). Osteochondral defect repair with autologous bone marrow-derived mesenchymal stem cells in an injectable, in situ, cross-linked synthetic extracellular matrix. *Tissue Engineering*, 12(12), 3405–3416. <http://dx.doi.org/10.1089/ten.2006.12.3405>
- Liu, Z., & Yao, P. (2015). Injectable thermo-responsive hydrogel composed of xanthan gum and methylcellulose double networks with shear-thinning property. *Carbohydrate Polymers*, 132, 490–498. <http://dx.doi.org/10.1016/j.carbpol.2015.06.013>
- Malda, J., Visser, J., Melchels, F. P., Jüngst, T., Hennink, W. E., Dhert, W. J. A., & Huttmacher, D. W. (2013). 25th anniversary article: engineering hydrogels for biofabrication. *Advanced Materials*, 25(36), 5011–5028. <http://dx.doi.org/10.1002/adma.201302042>
- Na, K., Kim, S., Woo, D., Sun, B., Yang, H., Chung, H., & Park, K. (2007). Synergistic effect of TGFβ-3 on chondrogenic differentiation of rabbit chondrocytes in thermo-reversible hydrogel constructs blended with hyaluronic acid by in vivo test. *Journal of Biotechnology*, 128(2), 412–422. <http://dx.doi.org/10.1016/j.jbiotec.2006.09.025>
- Ni, Y., Tang, Z., Cao, W., Lin, H., Fan, Y., Guo, L., & Zhang, X. (2015). Tough and elastic hydrogel of hyaluronic acid and chondroitin sulfate as potential cell scaffold materials. *International Journal of Biological Macromolecules*, 74, 367–375. <http://dx.doi.org/10.1016/j.ijbiomac.2014.10.058>
- Oudshoorn, M. H. M., Rissmann, R., Bouwstra, J. A., & Hennink, W. E. (2006). Synthesis and characterization of hyperbranched polyglycerol hydrogels. *Biomaterials*, 27(32), 5471–5479. <http://dx.doi.org/10.1016/j.biomaterials.2006.06.030>
- Oudshoorn, M. H. M., Rissmann, R., Bouwstra, J. A., & Hennink, W. E. (2007). Synthesis of methacrylated hyaluronic acid with tailored degree of substitution. *Polymer*, 48(7), 1915–1920. <http://dx.doi.org/10.1016/j.polymer.2007.01.068>
- Oudshoorn, M. H. M., Penterman, R., Rissmann, R., Bouwstra, J. A., Broer, D. J., & Hennink, W. E. (2007). Preparation and characterization of structured hydrogel microparticles based on cross-linked hyperbranched polyglycerol. *Langmuir*, 23(23), 11819–11825. <http://dx.doi.org/10.1021/la701910d>
- Roughley, P. J., & Mort, J. S. (2014). The role of aggrecan in normal and osteoarthritic cartilage. *Journal of Experimental Orthopaedics*, 1, 8. <http://dx.doi.org/10.1186/s40634-014-0008-7>
- Sawatjui, N., Damrongruang, T., Leeansaksiri, W., Jearanaikoon, P., Hongeng, S., & Limpiboon, T. (2015). Silk fibroin/gelatin-chondroitin sulfate-hyaluronic

- acid effectively enhances in vitro chondrogenesis of bone marrow mesenchymal stem cells. *Materials Science and Engineering: C*, 52, 90–96. <http://dx.doi.org/10.1016/j.msec.2015.03.043>
- Sawatjui, N., Damrongrungruang, T., Leeansaksiri, W., Jearanaikoon, P., & Limpaiaboon, T. (2014). Fabrication and characterization of silk fibroin–gelatin/chondroitin sulfate/hyaluronic acid scaffold for biomedical applications. *Materials Letters*, 126, 207–210. <http://dx.doi.org/10.1016/j.matlet.2014.04.018>
- Schuurman, W., Klein, T. J., Dhert, W. J. A., van Weeren, P. R., Hutmacher, D. W., & Malda, J. (2015). Cartilage regeneration using zonal chondrocyte subpopulations: a promising approach or an overcomplicated strategy? *Journal of Tissue Engineering and Regenerative Medicine*, 9(6), 669–678. <http://dx.doi.org/10.1002/term.1638>
- Steinmetz, N. J., & Bryant, S. J. (2012). Chondroitin sulfate and dynamic loading alter chondrogenesis of human MSCs in PEG hydrogels. *Biotechnology and Bioengineering*, 109(10), 2671–2682. <http://dx.doi.org/10.1002/bit.24519>
- Toh, W. S., Lim, T. C., Kurisawa, M., & Spector, M. (2012). Modulation of mesenchymal stem cell chondrogenesis in a tunable hyaluronic acid hydrogel microenvironment. *Biomaterials*, 33(15), 3835–3845. <http://dx.doi.org/10.1016/j.biomaterials.2012.01.065>
- Varghese, S., Hwang, N. S., Canver, A. C., Theprungsirikul, P., Lin, D. W., & Elisseeff, J. (2008). Chondroitin sulfate based niches for chondrogenic differentiation of mesenchymal stem cells. *Matrix Biology*, 27(1), 12–21. <http://dx.doi.org/10.1016/j.matbio.2007.07.002>
- Vermonden, T., Besseling, N. A. M., van Steenbergen, M. J., & Hennink, W. E. (2006). Rheological studies of thermosensitive triblock copolymer hydrogels. *Langmuir*, 22(24), 10180–10184. <http://dx.doi.org/10.1021/la062224m>
- Vermonden, T., Fedorovich, N. E., van Geemen, D., Alblas, J., van Nostrum, C. F., Dhert, W. J. A., & Hennink, W. E. (2008). Photopolymerized thermosensitive hydrogels: synthesis, degradation, and cytocompatibility. *Biomacromolecules*, 9(3), 919–926. <http://dx.doi.org/10.1021/bm7013075>
- Vermonden, T., Jena, S. S., Barriet, D., Censi, R., van der Gucht, J., Hennink, W. E., & Siegel, R. A. (2010). Macromolecular diffusion in self-assembling biodegradable thermosensitive hydrogels. *Macromolecules*, 43(2), 782–789. <http://dx.doi.org/10.1021/ma902186e>
- van Dijk-Wolthuis, W. N. E., Franssen, O., Talsma, H., van Steenbergen, M. J., Kettenes-van den Bosch, J. J., & Hennink, W. E. (1995). Synthesis, characterization, and polymerization of glycidyl methacrylate derivatized dextran. *Macromolecules*, 28(18), 6317–6322. <http://dx.doi.org/10.1021/ma00122a044>
- van Dijk-Wolthuis, W. N. E., Hoogeboom, J. A. M., van Steenbergen, M. J., Tsang, S. K. Y., & Hennink, W. E. (1997). Degradation and release behavior of dextran-based hydrogels. *Macromolecules*, 30(16), 4639–4645. <http://dx.doi.org/10.1021/ma9704018>
- van Dijk-Wolthuis, W. N. E., Kettenes-van den Bosch, J. J., van der Kerk-van Hoof, A., & Hennink, W. E. (1997). Reaction of dextran with glycidyl methacrylate: an unexpected transesterification. *Macromolecules*, 30(11), 3411–3413. <http://dx.doi.org/10.1021/ma961764v>
- van Dijk-Wolthuis, W. N. E., van Steenbergen, M. J., Underberg, W. J. M., & Hennink, W. E. (1997). Degradation kinetics of methacrylated dextrans in aqueous solution. *Journal of Pharmaceutical Sciences*, 86(4), 413–417. <http://dx.doi.org/10.1021/js9604220>
- Wang, L.-F., Shen, S.-S., & Lu, S.-C. (2003). Synthesis and characterization of chondroitin sulfate-methacrylate hydrogels. *Carbohydrate Polymers*, 52(4), 389–396. [http://dx.doi.org/10.1016/s0144-8617\(02\)00328-4](http://dx.doi.org/10.1016/s0144-8617(02)00328-4)
- Wei, J., Wang, J., Su, S., Wang, S., & Qiu, J. (2015). Tough and fully recoverable hydrogels. *J. Mater. Chem. B*, 3(26), 5284–5290. <http://dx.doi.org/10.1039/c5tb00504c>
- Yoo, H. S., Lee, E. A., Yoon, J. J., & Park, T. G. (2005). Hyaluronic acid modified biodegradable scaffolds for cartilage tissue engineering. *Biomaterials*, 26(14), 1925–1933. <http://dx.doi.org/10.1016/j.biomaterials.2004.06.021>
- Zhang, L., Li, K., Xiao, W., Zheng, L., Xiao, Y., Fan, H., & Zhang, X. (2011). Preparation of collagen-chondroitin sulfate-hyaluronic acid hybrid hydrogel scaffolds and cell compatibility in vitro. *Carbohydrate Polymers*, 84(1), 118–125. <http://dx.doi.org/10.1016/j.carbpol.2010.11.009>